

QC
996
.T33
no.71



A Technical Memorandum NWS NMC 71

A PROCEDURE TO REDUCE NORTHWARD DRIFT OF TROPICAL STORMS IN A NUMERICAL MODEL

National Meteorological Center
Washington, D. C.
July 1992

**U.S. DEPARTMENT OF
COMMERCE**

National Oceanic and
Atmospheric Administration

National Weather
Service

NOAA TECHNICAL MEMORANDUMS

National Meteorological Center
National Weather Service, National Meteorological Center Series

The National Meteorological Center (NMC) of the National Weather Service (NWS) produces weather analyses and forecasts for the Northern Hemisphere. Areal coverage is being expanded to include the entire globe. The Center conducts research and development to improve the accuracy of forecasts, to provide information in the most useful form, and to present data as automatically as practicable.

NOAA Technical Memorandums in the NWS NMC series facilitate rapid dissemination of material of general interest which may be preliminary in nature and which may be published formally elsewhere at a later date. Publications 34 through 37 are in the former series, Weather Bureau Technical Notes (TN), National Meteorological Center Technical Memoranda; publications 38 through 48 are in the former series ESSA Technical Memoranda, Weather Bureau Technical Memoranda (WBTM). Beginning with 49, publications are now part of the series, NOAA Technical Memorandums NWS.

Publications listed below are available from the National Technical Information Service (NTIS), U.S. Department of Commerce, Sills Bldg., 5285 Port Royal Road, Springfield, VA 22161. Prices on request. Order by accession number, (given in parentheses).

Weather Bureau Technical Notes

- TN 22 NMC 34 Tropospheric Heating and Cooling for Selected Days and Locations over the United States During Winter 1960 and Spring 1962. Philip F. Clapp and Francis J. Winninghoff, 1965, 18 pp. (PB-170-584)
- TN 30 NMC 35 Saturation Thickness Tables for the Dry Adiabatic, Pseudo-adiabatic, and Standard Atmospheres. Jerrold A. LaRue and Russell J. Younkin, January 1966, 18 pp. (PB-169-382)
- TN 37 NMC 36 Summary of Verification of Numerical Operational Tropical Cyclone Forecast Tracks for 1965. March 1966, 6 pp. (PB-170-410)
- TN 40 NMC 37 Catalog of 5-Day Mean 700-mb. Height Anomaly Centers 1947-1963 and Suggested Applications. J. F. O'Conner, April 1966, 63 pp. (PB-170-376)

ESSA Technical Memoranda

- WBTM NMC 38 A Summary of the First-Guess Fields Used for Operational Analyses. J. E. McDonell, February 1967, 17 pp. (AD-810-279)
- WBTM NMC 39 Objective Numerical Prediction Out to Six Days Using the Primitive Equation Model--A Test Case. A. J. Wagner, May 1967, 19 pp. (PB-174-920)
- WBTM NMC 40 A Snow Index. R. J. Younkin, June 1967, 7 pp. (PB-175-641)
- WBTM NMC 41 Detailed Sounding Analysis and Computer Forecasts of the Lifted Index. John D. Stackpole, August 1967, 8 pp. (PB-175-928)
- WBTM NMC 42 On Analysis and Initialization for the Primitive Forecast Equations. Takashi Nitta and John B. Hovermale, October 1967, 24 pp. (PB-176-510)
- WBTM NMC 43 The Air Pollution Potential Forecast Program. John D. Stackpole, November 1967, 8 pp. (PB-176-949)
- WBTM NMC 44 Northern Hemisphere Cloud Cover for Selected Late Fall Seasons Using TIROS Neph analyses. Philip F. Clapp, December 1968, 11 pp. (PB-186-392)
- WBTM NMC 45 On a Certain Type of Integration Error in Numerical Weather Prediction Models. Hans Okland, September 1969, 23 pp. (PB-187-795)
- WBTM NMC 46 Noise Analysis of a Limited-Area Fine-Mesh Prediction Model. Joseph P. Gerrity, Jr., and Ronald D. McPherson, February 1970, 81 pp. (PB-191-188)
- WBTM NMC 47 The National Air Pollution Potential Forecast Program. Edward Gross, May 1970, 28 pp. (PB-192-324)
- WBTM NMC 48 Recent Studies of Computational Stability. Joseph P. Gerrity, Jr., and Ronald D. McPherson, May 1970, 24 pp. (PB-192-979)

NOAA Technical Memorandums

- NWS NMC 49 A Study of Non-Linear Computational Instability for a Two-Dimensional Model. Paul D. Polger, February 1971, 22 pp. (COM-71-00246)
- NWS NMC 50 Recent Research in Numerical Methods at the National Meteorological Center. Ronald D. McPherson, April 1971, 35 pp. (COM-71-00595)
- NWS NMC 51 Updating Asynoptic Data for Use in Objective Analysis. Armand J. Desmarais, December 1972, 19 pp. (COM-73-10078)
- NWS NMC 52 Toward Developing a Quality Control System for Rawinsonde Reports. Frederick G. Finger and Arthur R. Thomas, February 1973, 28 pp. (COM-73-10673)

(continued on inside back cover)



QC
996
.T33
no. 71

A Procedure to Reduce Northward Drift of Tropical Storms in a Numerical Model



Makut B. Mathur and Alan M. Shapiro

Washington, D.C.
July 1992

**UNITED STATES
DEPARTMENT OF COMMERCE**

**Barbara Hackman Franklin
Secretary**

**National Oceanic and
Atmospheric Administration**

**John A. Knauss
Under Secretary**

**National Weather
Service**

**Elbert W. Friday, Jr.
Assistant Administrator**



**A procedure to reduce northward drift of tropical storms
in a numerical model**

Mukut B. Mathur

(National Meteorological Center, Washington D.C.)

and

Alan M. Shapiro ¹

(UCAR Visiting Scientist, National Meteorological Center, Washington D.C)

¹ Present Affiliation : CAPS, University of Oklahoma, Norman, OK

ABSTRACT

Operational primitive equation models often predict hurricane tracks that lie to the right of the observed motion. Such a bias in the National Meteorological Center's Quasi-Lagrangian Model (QLM) is most pronounced for the storms that moved westward. It is shown that a westward displacement of the storm's circulation in the initial analysis significantly contributes to this erroneous motion to the right of the observed track in the QLM.

A procedure to reduce this bias for westward moving storms is presented. It consists of imposing a secondary circulation (a dipole) over the initial storm area. The cyclonic (anticyclonic) lobe of the dipole is centered to the south (north) of the observed track. The use of this dipole procedure resulted in a substantial improvement in the forecast track throughout the 72 hour period in several cases.

1 Background

The Quasi-Lagrangian Model (QLM) of the National Meteorological Center (NMC) provides numerical track forecast guidance for tropical storms in the Atlantic Ocean, the Gulf of Mexico, and the eastern Pacific Ocean. The QLM is integrated in the cases of rapidly developing depressions, tropical storms and hurricanes. We are not concerned here with the forecast of a tropical cyclone's intensity. A storm in this paper refers to a disturbance in any of the above stages of a tropical cyclone.

The QLM employs a set of primitive equations with σ (= pressure / surface pressure) as a vertical coordinate, a horizontal grid of 111 x 111 points with a 40 km spacing, and 16 vertical layers. The center of the grid coincides with the initial position of the observed storm. Because of lack of observations near a storm's center, a storm's circulation is often not well analyzed operationally. Therefore, an idealized symmetric vortex whose structure depends on five parameters (the central pressure p_c , pressure of the outermost closed isobar p_b (reckoned with a precision of 1 mb), mean distance r_{max} (which is also referred to below as the size or radius of a storm) of the outermost closed isobar from the center, storm center latitude c_{lat} and longitude c_{lon}) is merged into the NMC's Global Aviation (AVN) analysis to simulate a storm in the QLM's initial state. These parameters are derived by the National Hurricane Center (NHC) from their analysis and are transmitted to the NMC. The idealized vortex has a warm core and nearly the same size and intensity as the observed storm (except that the central pressure is set to 970 mb whenever p_c is less than this value because large gradients can not be prescribed well with the use of a 40 km grid spacing). The winds are cyclonic in the lower and middle troposphere and anticyclonic in the upper troposphere. The vortex and the AVN analysis are first projected separately on the QLM grid and then merged using the relation:

$$X_m = wX_v + (1 - w)X_a$$

where, X is one of the variable (a horizontal component of the wind, the virtual potential temperature, the mixing ratio, or the surface pressure). The subscripts m, v and a denote a field in the merged data, vortex and analysis, respectively. The vortex is projected so that the vortex center coincides with the center of the QLM grid. The weight function w is given by:

$$w = \cos\left(\frac{\pi r}{2 r_{\max}}\right) \quad r < r_{\max},$$

$w = 0$ otherwise.

Here r is the distance from the observed center. The lateral boundary conditions for the QLM are derived from the AVN model's forecast on the σ surfaces. A description of the QLM is given in Mathur (1983, 1991) and the specification of the initial vortex including the merging procedure is provided in Mathur 1988.

During the 1988 hurricane season, no systematic bias in the QLM forecast storm tracks was noticed for the storms that moved northward or northeastward. However, the predicted track was located to the north of the observed track in many cases where the observed motion of a storm was towards the west (between angles 210° and 310° reckoned clockwise from the north). The erroneous northward drift generally occurred in the first 24 hours of a forecast. It should be noted that the operational position of the storm center that was provided by the NHC for the QLM forecast is referred to as the observed storm center throughout this paper.

As an example, we show (Fig. 1.) the observed and predicted track of hurricane Gilbert for the initial time 12 GMT 10 September 1988. The QLM uses the maximum relative vorticity at 850 mb as the locus of the storm's center. The storm in the model forecast moved north-northwestward in the first 24 h, then, at later times, nearly paralleled the observed track. The northward drift of storms has also been noted in other tropical cyclone models (e.g., see Hodur 1989, and Iwasaki et al. 1987.)

The northward drift of storms due to the variation in the Coriolis parameter has been investigated in several studies. Rossby (1948) suggested that an initially symmetric cyclonic vortex would accelerate to the north on a β -plane due to the differential strength of the Coriolis parameter. As a refinement of this conception, the barotropic studies of Chan and Williams (1987) and Fiorino and Elsberry (1989) suggested that an initially symmetric vortex is first distorted by differential advection of earth's vorticity which sets up a pair of counter-rotating β -gyres, a cyclonic gyre is developed to the west and an anticyclonic gyre to the east of the

vortex center. The vortex is then advected by the flow associated with the gyres. The net effect is for an initially symmetric vortex to move north-westward in the northern hemisphere. This so called β -drift (where $\beta = \partial f/\partial y$) increases with the size of the storms.

Mathur (1986,1987) conducted several experiments to further study the motion of storms utilizing a 10 layer version of the QLM. A grid spacing of 40 km, and idealized initial vortices of different size and intensity with or without a zonal basic current were used. The initial vortex intensified into a hurricane in all cases. (The integration were carried out to 120 h for no basic current cases and to 72 h for uniform basic current cases). The northward displacement when averaged over the entire forecast period was greater for a larger (and/or stronger) initial vortex than for a smaller (and/or weaker) initial vortex. Thus, the northward drift depended on both the size and the intensity of the initial vortex.

On the other hand in the operational QLM forecasts, a larger and stronger storm (Hurricane Gilbert, Fig. 2), drifted less northward than a smaller storm (Tropical storm Joan, Fig. 3). In view of the experimental studies cited above, this difference in the northward drift can not be explained solely by the variation in the Coriolis parameter.

We therefore examined the AVN analysis (interpolated to the QLM grid) as a possible cause of the spurious northward drift. The center of the storm circulation in both cases considered above is located to the west of the observed center (Fig. 4). Recall that the QLM's initial state is designed so that the center of a storm coincides with the observed center. When a storm's center is displaced in the analysis, a part of the symmetric component of the analyzed circulation will appear as an asymmetric circulation over the central vortex area in the merged state. This asymmetric circulation may steer the storm model vortex. The displacement is larger and the analyzed southerly winds over and near the observed center area are stronger in Joan than in Gilbert (Fig. 4). Therefore a greater northward displacement is anticipated in the Joan case than in the Gilbert case. The QLM predicted storm tracks depicted in Figs. 2 and 3 demonstrate that this was the case.

Other case studies also suggest that the erroneous northward drift of the storms in the QLM is largely due to a systematic westward displacement of the cyclonic circulation in the analysis relative to the observed storm center. As a consequence of this displacement, a southerly flow is

analyzed over the observed storm location. Such a westward displacement of tropical disturbances in the NMC operational analyses has been noted by C. J. Neumann and S. Lord (personal communications).

One may therefore anticipate that the erroneous northward drift in the QLM for westward moving storms should be reduced by decreasing a storm's location error in the AVN analysis. Andersson and Hollingsworth (1988), and M. Ueno (personal communication) have attempted to improve the structure and location of storms in a global analysis by introducing bogus soundings in the region of storms. The bogus data are derived from an empirical symmetric vortex representing the structure of a mean hurricane that has been adjusted based on a few observed parameters. Different specifications of the vortex and levels for inserting bogus data are used in the two studies. In the Andersson and Hollingsworth study, the first guess-fields (six hour forecast from the previous cycle) truncated at T20 are added to the bogus vortex to represent the large-scale circulation. Because of the coarse global analysis grid spacing (of the order of a few hundred kilometers), storm location errors can be more than 100 km even with the use of bogus data.

Procedures to reduce the storm location error to a tolerably small value (ideally zero) in the AVN analysis have not yet been developed. We have therefore considered techniques to compensate for the location error and thus reduce the northward drift in the model track predictions. Use of a method in which a dipole was imposed on the idealized vortex led to a substantial improvement in forecast tracks. The dipole is described in section 2, and results showing improved track forecasts are presented in section 3. In contrast to some earlier reports (e.g., Pike 1972) where a uniform steering current is imposed, our procedure is more general, the current varies in the horizontal and the variation is controlled by a few parameters.

2 Specification of a dipole

We superpose a secondary circulation resembling a dipole over the primary symmetric vortex. The free parameters appearing in this description will be related to analyzed storm parameters in the next section. The dipole is specified in a Cartesian coordinate system (X, Y) with the origin at the storm's center. The negative X axis is directed along an angle γ measured clockwise from the axis Y' , where (X', Y') are the coordinate axes on the QLM grid (see Fig. 5). The

maximum dipole wind speed, u_{max} , is at the observed vortex center and is directed along the negative X axis. The anticyclonic (cyclonic) circulation center of the dipole is located along the positive (negative) Y axis.

The streamfunction that describes the dipole perturbation is:

$$\psi = A \exp \{-(a|x| + b|y|)\} \sin(y/l) \quad (1)$$

where a, b, l, and A are disposable parameters. x and y are the distances along the coordinate axis X and Y respectively. Differentiating Eq. (1) with respect to y and x gives, respectively, the velocity components directed along and perpendicular to the dipole axis.

$$u = -A \exp \{-(a|x| + b|y|)\} \{-by/|y| \sin(y/l) + \cos(y/l)/l\} \quad (2)$$

$$v = -A \exp \{-(a|x| + b|y|)\} ax/|x| \sin(y/l) \quad (3)$$

Since the maximum u-component of the dipole velocity is at the storm center, (x=0, y=0),

$$u_{max} = -A/l \quad (4)$$

Since the dipole streamfunction is constant (zero) along the coordinate values $y = n\pi l$ (for integer n), the y-component of wind vanishes along these coordinate lines. For n=1, $|y| = \pi l$, and the u-component takes the value at x=0

$$u_{edge} = A \exp(-b\pi l) / l \quad (5)$$

This equation may be rewritten as an expression for b

$$b = -\ln\{|lu_{edge}/A|\} / l \pi \quad (5)$$

The parameter L is defined such that at x=0 and y=L (or -L) both u and v are zero, i.e., the

coordinates (0,L) and (0,-L) define the centers of the dipole lobes. Evaluating (2) at the dipole lobe centers gives the formula

$$\tan(L/l) = 1/bl \quad (6)$$

A simple expression for b results from inserting (4) into (5)

$$b = - \ln \{ |u_{edge}/u_{max}| \} / l \pi \quad (7)$$

Substituting (7) into (6) provides a simple expression for l

$$l = - L / \tan^{-1} \{ \pi / \ln |u_{edge}/u_{max}| \} \quad (8)$$

The adjustment in the height field (z) required by the insertion of the dipole streamfunction is specified as a simple geostrophic increment to the primary vortex height field

$$z = f\psi/g \quad ,$$

where g is the acceleration due to gravity.

In summary, the analytic perturbation dipole has five free parameters: a, b, A, l and γ . It was convenient to specify a, γ , L, u_{max} , and u_{edge} , and compute l from (8), A from (4), and the attenuation factor, b, from (7).

The original purpose of the present work was to use a dipole to impose steering winds based on observed motion (persistence) over the idealized vortex on the QLM model grid. A dipole was selected for two reasons: (1) to study the impact of nonuniform steering current on the motion of storms. We envisioned that a current (having nearly the same direction as the observed storm motion) in a narrow zone (zonal width of the order of r_{max}) with the maximum wind at the storm's center may give most improvement in track forecasts. Note that the horizontal variation, the strength, and the width of the current can be adjusted by a suitable choice of all or some of the five parameters. The variation in the vertical can be taken into account by using vertical weighting functions. (2) The use of a dipole may reduce the northward motion of westward

moving storms because the relative vorticity in the dipole is negative to the north and positive to the south of the storm center in these cases. The change in relative vorticity due to the advection of the dipole relative vorticity by the symmetric storm winds is thus of an opposite sense to the change due to the advection of planetary vorticity.

Because only limited computer resources were available, it was not possible to study the impact on the forecast track of varying each free parameter while keeping the remaining parameters fixed. Instead, a narrow steering current zone was specified by setting a and u_{edge} as a fraction of b and u_{max} respectively, and specifying L as a value smaller than r_{max} . Various values of u_{max} between 2 and 25 m/s and of γ within 40° of the observed storm motion were used. Only the three cases of Figs. (1)-(3) were considered. In an experiment γ was set to the observed direction of a storm, and u_{max} was evaluated so that the mean wind over a circular area of radius L matched the observed storm speed. Although this general procedure did improve the forecast, a comparison of experimental results showed that a fixed value of γ of 270° and u_{max} specified by Eq. (9) yielded the best forecasts for the westward moving storms (observed motion between $210^\circ - 310^\circ$). Attempts are currently underway to optimally tune the parameters for the general dipole case. The remainder of this paper is concerned with the experimental design and numerical results corresponding to γ fixed at 270° .

a. Dipole parameters

The above experiments also showed that the reduction in the northward drift of a storm with the use of a dipole depends on the strength and the width of the easterlies (case $\gamma = 270^\circ$) between the dipole lobes. This dependence may be expected as the advection of the vortex would depend on the width and strength of the steering current (see also section 3b). The northward drift in the 1988 operational QLM forecast cases was large for storms that were small in size and for those that were located at low latitudes. The empirical relations for u_{max} in (9), and L in (10) were formulated taking the above dependence of drift on the latitude and size of a storm. The numerical coefficients were determined as optimal values for reducing the drift in three cases in Figs. 1-3.

u_{max} , u_{edge} , a and L were defined by the following relations.

$$u_{\max} = C / (c_{lat} RR) \quad (9)$$

$$u_{edge} = -.8 u_{\max}$$

$$a = 0.6 b$$

$$L = \text{MIN} (r_{\max} - 50 , 600) \quad (10)$$

Here $C = -136000$ km m/s, $RR = \text{MAX} (r_{\max} , 500)$. Here r_{\max} is expressed in kilometers. Noise developed in a few 72 h forecasts where a value of u_{\max} less than -20 m/s was used. Therefore, u_{\max} is set to -20 m/s, if it is less than this value.

Use of a value of L greater than 600 km for a storm with r_{\max} larger than 650 km (e.g., Gilbert) resulted in excessive southward displacement of the forecast center, an upper limit of 600 km is therefore assigned to L .

With the above specifications, the wind over the storm center is from the east. The easterlies decrease in all directions from the center, and eventually change to westerlies to the north (south) of the anticyclonic (cyclonic) lobe centers. The velocity and height fields of the dipole in the idealized vortex area (i.e., within a radius r_{\max} of the observed storm center) were added to the QLM initial state in all vertical layers. It is shown in section 3a that the predicted storm direction in the QLM has nearly zero correlation with the direction of asymmetric winds above 500 mb. Note that the initial asymmetric wind consist of a vector sum of the dipole wind and the asymmetric component that is derived from the analysis as a result of merging of vortex into the analysis. In a very few cases, the QLM was also integrated using a weighted dipole, where the weight was set to 1 up to level 10 ($\sigma = .472$), and then linearly reduced upward with a value of 0.2 at the top most layer. The forecast using the weighted dipole was not significantly different from the case when weights are set to unity at all levels.

An example of a dipole structure is provided in Fig. 6. The dipole streamfunction (1) for Gilbert on 12 GMT 14 September ($r_{\max} = 740$ km) is shown in Fig. 6a. The winds at 850 mb without a dipole (Fig. 6b) are nearly axisymmetric. The imposition of the dipole (Fig. 6c) results in stronger winds to the north and weaker winds to the south compared with the case without a dipole.

3 Numerical results

Results from 72 h integrations of the QLM with a dipole for nine cases in which a northward drift was predicted in the operational QLM are now considered. It is shown that a significant improvement in forecast mean track errors is obtained with the use of a dipole (section 3a). Predictions for three representative cases are also presented (section 3b-3d). Operational implementation of the dipole procedure is discussed in section 3e.

a. Mean track forecast errors

The QLM was integrated using a dipole for the cases in which the observed storm motion was towards the west (between 210° and 310°) and the AVN forecasts that are required for the QLM lateral boundary conditions were available. A list of these cases with the observed and predicted (without a dipole) motion of storms during the first 12 h are presented in Table 1. The analyzed winds averaged over square areas inscribing circles of radii of r_{max} , $2 r_{max}$, and $3 r_{max}$ for the initial time are also shown. The vertical averaging was carried out using only the data for layers 1 ($\sigma = 1$) to 10 ($\sigma = .472$), because we have noticed that the motion of storms in the QLM has nearly zero correlation with winds above the 500 mb level. For example, we have examined the predicted asymmetric part of the wind over the central storm area (of radius $2 - 3^\circ$ latitude) in a few cases at different forecast hours. The direction of asymmetric winds below 500 mb is often within $20 - 30^\circ$ of the predicted direction of storm motion, while the wind direction above 500 mb differed by nearly 180° from the predicted storm motion.

Inspection of Table 1 reveals two points of interest. First, note that the direction of QLM vortex motion is correlated more with the $1 r_{max}$ average analyzed wind direction than with the $2 r_{max}$ or $3 r_{max}$ averages. This is consistent with the non-divergent barotropic model results of Smith et al. (1990) in which the environmental wind averaged over the innermost of the $0 - 1^\circ$, $1 - 3^\circ$, $3 - 5^\circ$, $5 - 7^\circ$, latitude annular regions (centered on the vortex vorticity center) yielded the best agreement with the motion of the vorticity center. Secondly, the observed motion is in closer agreement with the $3 r_{max}$ average analyzed wind direction except in the cases when the difference between the observed and predicted direction of motion is small. In the latter cases, both directions are close to the $1 r_{max}$ average. The difference between the vortex speed in the QLM and the average analyzed $1 r_{max}$ speed is generally 2 m/s or less. This

implies that the QLM vortex may be steered by its immediate model environment, at least in the first 12 hours, whether or not it is a correct representation of the real atmosphere. When the observed direction of storm motion does not agree with the $1/r_{\max}$ average then one can anticipate that the model vortex will drift significantly from the observed storm track.

The mean QLM forecast track error is significantly reduced by including a dipole perturbation to the wind and pressure fields (Table 2). The greatest improvement in the storm track occurs at 72 hours where the mean error was reduced by 228 km. The mean error is reduced with the use of the dipole in the three representative cases by 228 km at 24 h, 128 km at 48h, and 194 km at 72 h. The reduction in mean error is also large in the rest of the six cases (independent sample), it is 148 km at 24 h (6 cases), 156 km at 48 h (5 cases), and 261 km at 72h (3 cases). Since some of the storms dissipated before 72 hours, the number of cases considered decreased with time.

An improvement in the forecast track with the use of a dipole occurred in all cases when the entire forecast period (72 h) is considered. However, the improvement differed considerably from one case to another. The largest improvement resulted for the case of Gilbert 12 GMT 10 September (Fig. 1), and the smallest improvement in the case of Joan 12 GMT 12 October (Fig. 3). A discussion of three track predictions including these latter two cases is now presented.

b. Case 1 : Gilbert 12 GMT 10 September 1988

As noted above, the storm's center in the operational QLM forecast (a case without the use of a dipole) for 12 GMT 10 September drifted northward in the first 24 hours (Fig. 1). Thereafter the center paralleled the observed track so that the track forecast errors were nearly constant at about 250 km during the 12 to 72 h period. The predicted track was located much closer to the observed track during the first 48 h when a dipole was used. Although the storm moved more rapidly towards the northwest in the forecast than indicated by the observations after 48 h, the location errors still remained smaller. Notice that the time and location of landfall over Jamaica are predicted well when the dipole is included.

c. Case 2 : Gilbert 12 GMT 14 September

The forecast speeds of the storm both without and with the dipole included were slower than observed during the first 12 hours (Fig. 2). The center was located very close to the observed

center at 24 and 36 h in the forecast including the dipole, whereas the storm center is about 200 km to the east of the observed center at these hours in the forecast without the dipole. Gilbert was observed to drift towards the northwest after 36 h; this drift began after 24 h in forecast without the dipole and only after 48 h with the dipole. Consequently, the storm center at 48 h in with (without) the dipole is located to the south (north) of the observed center. The time and the location of landfall over Mexico are better predicted with the dipole compared to without the dipole.

Further insight into the behaviour of storm with and without a dipole can be gained by comparing the terms in the vorticity equation in the two cases. Neglecting the diffusive terms the tendency equation for relative vorticity (pressure coordinates) may be written as:

$$\begin{aligned} \frac{\partial \zeta}{\partial t} = & - \left(u' \frac{\partial \zeta}{\partial x} + v' \frac{\partial \zeta}{\partial y} \right) - \omega \left(\frac{\partial \zeta}{\partial p} \right) \\ & - (\zeta + f) \left(\frac{\partial u'}{\partial x} + \frac{\partial v'}{\partial y} \right) \\ & - \left(\frac{\partial v'}{\partial p} \frac{\partial \omega}{\partial x} - \frac{\partial u'}{\partial p} \frac{\partial \omega}{\partial y} \right) - v' \frac{\partial f}{\partial y} \end{aligned}$$

Here ζ is the vertical component of relative vorticity, f is the Coriolis parameter, ω is the vertical p-velocity, and u' and v' are horizontal components of wind in the QLM coordinate system. The total tendency is the sum of five terms on the right hand side; these terms are the horizontal and vertical advection of vorticity, divergence, twisting and β - term respectively.

Here

$$\beta = \frac{\partial f}{\partial y}$$

In an observational study Chan (1984) showed that tropical cyclones nearly move along the axis connecting the vorticity tendency minimum behind the storm to the vorticity tendency maximum ahead of the storm. The total tendency at 6h in the dipole and no dipole cases at 850

mb (Figs. 7a and 7c) shows that the minimum to maximum value axis is oriented east-west in the dipole case, and southeast-northwest in the no dipole case. The orientation of this axis in the horizontal advection term (the location of maximum and minimum centers are shown in the above figures) is nearly the same in both forecasts. Note that in both cases the two minimum centers (total and horizontal terms) nearly coincide, but the maximum center in the total tendency field is displaced to the south of the corresponding center in the horizontal advection field. This displacement of the maximum center is related to the location of the maximum in the stretching term to the southwest of the storm center (Figs. 7b and 7d). The maximum value in the horizontal advection field is 213 (units: 10^{-10} s^{-2}) in the dipole case and 232 in the no dipole case. The stretching term is of nearly the same magnitude as the horizontal advection term in the dipole case but is smaller in the no dipole case. The contribution from other terms to the total tendency is relatively small except that for the vertical advection term. The maximum in vertical advection term (not shown) in both cases has nearly the same magnitude as the minimum of the stretching term and the two centers nearly coincide. The location of the minimum in the total tendency is therefore not much displaced from the corresponding location of the minimum in the horizontal advection field in both predictions, and the maximum center in total is located closer to maximum center of the stretching term in the dipole case than in the no dipole case. The distribution and magnitude of the various terms are not the same in the two cases, and the stretching and the vertical advection term contribute more to the motion of the storm in the dipole than in the no dipole case.

d. Case 3 : Joan 12 GMT 12 October 1988

The operational QLM forecasts for Joan from the initial times 00 and 12 GMT between 12 October and 23 October showed that an excessive northward drift occurred in many forecasts between the 12th and 17th. AVN forecasts needed for QLM boundary conditions were available in only two of these cases. The two cases are included in the mean forecast error comparison (Table. 1), and one (12th October) is discussed below.

This storm drifted northwestward in the QLM integrations (Fig. 3) without and with a dipole. The forecast track errors are, however, reduced throughout the 72 h period with the use of the dipole. The predicted tracks are parallel after 24 h, which suggests that the inclusion of a dipole impacted the forecast only during the first 24 h.

Joan also drifted northwestward in the AVN model's 36 h forecast (Fig. 8a) and at 72 h (Fig. 8b). The centers of the storm at these hours in the AVN and the QLM are close to each other. We conclude from this comparison that the extended northward drift in this case is due to errors in the analysis over a very large area surrounding this storm.

e. Operational implementation

The inclusion of the dipole procedure operationally is likely to provide an improved forecast track guidance in cases where a storm circulation is displaced in the analysis. Since there is currently a systematic westward bias in the analysis, we have restricted our attention in this paper to compensating for this particular problem. However, recent experiments performed with the QLM indicate that a significant improvement in storm track prediction can be attained in most cases with the application of a generalized dipole (Mathur 1991).

It should be noted that the analyzed circulation sometimes appears only as a trough. The displaced circulation often has a vertical tilt, and the maximum displacement often occurs at a higher level (usually 700 or 500 mb level). Because the structure of the displaced circulation (closed circulation or a trough, orientation of the trough axis associated with the circulation, and vertical tilt), and the distance of its center (or trough axis) from the observed center vary greatly from case to case, a satisfactory numerical procedure could not be developed to diagnose whether a storm is displaced in the analysis.

During the 1988 hurricane season, a westward moving storm drifted northward in the QLM forecast in a very large number (about 90%) of cases. The dipole procedure (section 2a) was therefore implemented for the 1989 season, since its inclusion is likely to improve the forecast track in a majority of westward moving storm cases. The NHC provided the expected direction of motion and speed of a storm in addition to the five parameters listed in section 1. A dipole was used if the direction was between 210° - 310° and the speed was greater than 1 m/s (It was anticipated that the latter requirement would exclude nearly stationary storms that are likely to recurve). The QLM without a dipole was run in parallel to the operational QLM (with dipole) in many 1989 westward moving storm cases. The forecast with the use of a dipole were superior to those without a dipole in a majority of cases. In a few cases where a northward drift did not

occur in the QLM without a dipole, the track forecast errors without a dipole were similar to those with a dipole. Cases of operational forecasts with the use of a dipole are presented in a separate report where 1989 season QLM forecast tracks are discussed (Mathur, 1991).

4 Discussion

Current operational primitive equation models often predict tropical storm tracks that are located to the right of the observed tracks. The largest such forecast errors in the QLM occurred for the westward moving storms. Three factors are thought to contribute to this erroneous northward motion in the model forecasts. First, a part of the drift could be due to the latitudinal variation in the Coriolis parameter. In previous QLM studies utilizing idealized symmetric storms with and without a uniform steering current, Mathur (1986, 1987) showed that the northward drift due to the β - effect was smaller in the first 24 hours than in the periods 24 - 48 and 48 - 72 h. This is because the gyres induced by the β - effect take some time to develop. Additionally Mathur found that larger (stronger) storms drifted further north than smaller (weaker) storms. On the other hand, the drift in many operational 1988 cases was larger in the first 24 h than in the later 24 h periods (e.g., Figs. 1 and 3). Also, a smaller and weaker storm (Joan, Fig. 3) moved further north than a larger and stronger storm (Gilbert, Fig. 2). Although the β - effect may have contributed to the northward drift, some other processes were undoubtedly also operating.

A second source of error is associated with a systematic displacement of the storm center in the analysis to the west of the observed center. In this case, the winds in the analysis have a significant southerly component over the observed storm area. Forecasts from several cases suggest that if the erroneous southerly flow is strong or its area is large compared to the model storm, then the storm in the QLM forecast is likely to be advected significantly northward during the first 24 hour. For instance, the analyzed southerly winds were stronger over the small storm (Joan) than over the large storm Gilbert. As a result, the smaller storm Joan drifted much farther to north than the stronger storm Gilbert in the first 24 h QLM forecasts.

Obviously, poorly analyzed fields over very large areas of the domain can also degrade the QLM forecast. This third source of error has not been fully investigated. However one may anticipate that when the large scale analysis is incorrect an erroneous "drift" from the observed

track may be large and may operate during all time periods. The continual northward drift of Joan in both the QLM and AVN forecasts for all time periods (section 3d) may have been due to improperly analyzed large scale features (a displaced vortex probably contributed to the 0-24 h track errors as well). If the analysis provides a good representation of large-scale atmospheric features but is deficient in the vicinity of the storm, one may expect good predictions of storm speeds and directions after an initial period of model storm drift. For instance, the track errors for the two Gilbert cases considered in section 3 level off at 24-36 h. Since the horizontal resolution of the analysis is of the order of a few hundred kilometers and the mean error during this period in the two cases is smaller (of the order of 200 km) than the resolution of the analysis, it may be assumed that the analyses in these two cases were good. This suggests that the so-called "steering" current over the observed storm area in the real atmosphere and over the predicted storm area in the QLM were in good agreement during the 24-72 h period.

Since the dipole wind and height fields are imposed only within the area occupied by the observed storm, it is unlikely that its inclusion would lead to a reduction in track forecast errors arising from large-scale analysis errors. The numerical results (section 3) suggest that the inclusion of a dipole reduces the northward drift arising from the erroneous southerly steering current that appears over the storm area in the QLM initial state (associated with a westward displacement of the observed vortex in the analysis). Recall that the dipole of section 2 introduces an easterly steering current over the storm area between the lobes (see Eq. 10 for the location of lobe centers) and that storm motion in the QLM is correlated well with the vertically averaged winds over a $1 r_{\max}$ area (see section 3 and Table 1). The inclusion of the dipole easterlies therefore leads to a more westward motion of a vortex.

The contribution of various terms in the propagation of the vorticity maximum at 850 mb (this maximum defines the storm center in the QLM) was also investigated in a case (section 3). The maximum in relative vorticity tendency is located to the south and to the west of the storm center in the dipole case compared to the no dipole case. The two terms which contribute the most in this displacement of the maximum tendency are the horizontal advection term and the stretching term. The maximum in the horizontal advection term in the dipole case is located to the south of the maximum in the no dipole case (Fig. 7). The stretching term is of the same order as the horizontal advection term in the dipole case and the maximum in this term is located to the southwest of the center. The stretching term is weaker in the no dipole case.

Smith et al. (1990) used a barotropic model on both f and β -*plane* and studied the motion of a symmetric vortex embedded initially in a southerly current that was prescribed using a west-east dipole. They varied the dipole scale to shift the asymmetric vorticity centers from the storm center. In the case the asymmetric vorticity was initially concentrated in the region of large shear in the tangential wind of the symmetric storm, the asymmetric vorticity underwent large distortion (wrapped around the storm center) and the storm initially stalled. This distortion became weaker as the asymmetric vorticity centers were displaced farther away from the region of the large tangential wind shear. We have not noticed any wrapping around of vorticity in our experiments, this may be due to the fact that the dipole lobes are initially located in the weak tangential wind shear near the storm boundary.

Andersson, E., and A. Hollingsworth, 1988: Typhoon bogus observations in the ECMWF data assimilation system. ECMWF Technical Memorandum No. 148, 25pp. [ECMWF, Shinfield Park, Reading, Berkshire RG2 9AX, England.]

Chan, J. C. L., 1984: An observational study of physical processes responsible for tropical cyclone motion. J. Atmos. Sci., 41, 1036-1048

Chan, J. C. L., and R. T. Williams, 1987: Analytical and numerical studies of the β -effect in tropical cyclone motion. Part I: Zero mean flow. J. Atmos. Sci., 44, 1257-1265.

Fiorino, M., and R. L. Elsberry, 1989: Some aspects of vortex structure related to tropical cyclone motion. J. Atmos. Sci., 46, 975-990.

Hodur, R. M., 1989: Tropical cyclone track prediction in a regional model. Extended Abstracts. 18th Conf. on Hurricanes and Tropical Meteorology, San Diego, Amer. Meteor. Soc., 174-175.

Iwasaki, T., H. Nakano, and M. Sugi, 1987: The performance of a typhoon track prediction model with cumulus parameterization. J. Meteor. Soc. Japan, 65, 555-57.

Mathur, M. B., 1983: A quasi-Lagrangian regional model designed for operational weather prediction. Mon. Wea. Rev., 111, 2087 - 2098.

-----, 1986: Application of quasi-Lagrangian model to hurricane prediction. Extended Abstracts. WMO/IUGG International Symposium on Short and Medium Range Numerical Weather Prediction. WMO/TD NO. 114, 461 - 464.

-----, 1987: Development of the NMC's high resolution hurricane model. Extended Abstracts, 17th Conf. on Hurricanes and Tropical Meteorology, Miami, Amer. Meteor. Soc., 60-63.

-----, 1988: The NMC Quasi-Lagrangian Hurricane Model. Technical Procedure Bulletin 377, National Weather Service, Silver Spring, Maryland. 10pp. [NOAA/NWS/NMC, Development Division, W/NMC2, WWB Room 204, Washington D.C. 20233.]

-----, 1991: The National Meteorological Center's Quasi-Lagrangian Model for Hurricane prediction. Mon. Wea. Rev., 119, 1419-1447.

Pike, A. C., 1972: Improved barotropic hurricane track prediction by adjustment of the initial wind field. NOAA Technical Memorandum NWS SR-66, National Weather Service, Silver Spring, Maryland. 17pp. [National Hurricane Center, 1320 S. Dixie Highway, Coral Gables, Fla. 33146.]

Rossby, C. G., 1948: On displacement and intensity changes of atmospheric vortices. J. Mar. Res., 7, 175-187.

Smith, R. K., W. Ulrich, and G. Dietachmayer, 1990: A numerical study of tropical cyclone motion using a barotropic model. I: The role of vortex asymmetries. Quart. J. Roy. Meteor. Soc., 116, 337-362.

Table 1. Observed and QLM predicted storm motion for the first 12 hours. Analyzed wind speed and direction averaged vertically over the model's first 10 sigma levels and horizontally over a square of sides $1r_{max}$, $2r_{max}$ and $3r_{max}$ are also presented. Direction is given in degrees reckoned clockwise from the north. Speed is given in m/s.

Storm name/date	Observed speed and direction	QLM vortex speed and direction	RMAX (km)	Averaged analysis wind speed and direction		
				$1r_{max}$	$2r_{max}$	$3r_{max}$
Gilbert						
12Z 9/10/88	283/6.8	332/7.2	370	308/8.4	295/6.9	284/5.6
00Z 9/12/88	284/8.3	329/7.1	555	317/5.7	293/4.8	282/3.5
12Z 9/14/88	288/7.5	277/4.3	740	300/5.8	316/3.1	12/1.3
12Z 9/15/88	287/5.2	281/2.7	740	300/4.1	319/2.6	42/0.8
Joan						
12Z 10/12/88	277/6.3	313/7.8	170	324/8.0	308/7.3	297/6.9
12Z 10/16/88	266/3.7	331/5.2	280	306/5.0	289/5.6	283/5.1
Fabio						
12Z 8/2/88	284/5.1	355/5.6	465	308/3.5	281/5.1	269/5.1
12Z 8/3/88	303/6.5	320/9.3	465	304/7.1	282/7.5	273/6.5
Uleki						
00Z 8/30/88	284/5.1	329/2.4	170	328/4.7	303/4.7	291/4.7

Table 2. Mean QLM forecast track errors (km) with and without a dipole.

Hour	No Dipole	Dipole	Cases
0	-	-	9
12	183	106	9
24	317	143	9
36	363	211	9
48	391	246	8
60	502	337	7
72	580	352	6

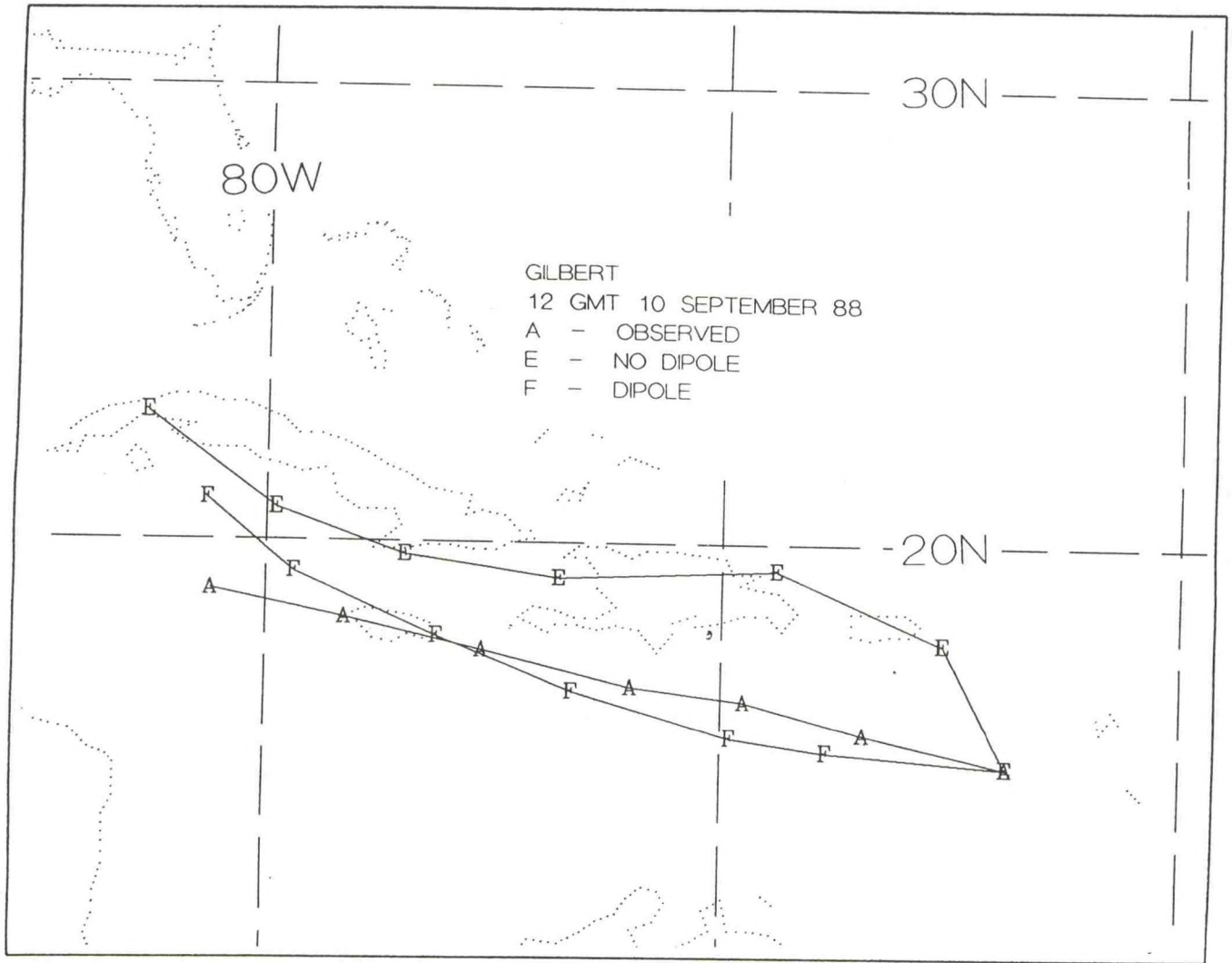


FIG. 1. Observed (A) and QLM predicted storm tracks (without (E) and with (F) a dipole) for Gilbert. Initial time is 12 GMT 10 Sept. 1988. Subsequent locations are shown at 12 hour intervals.

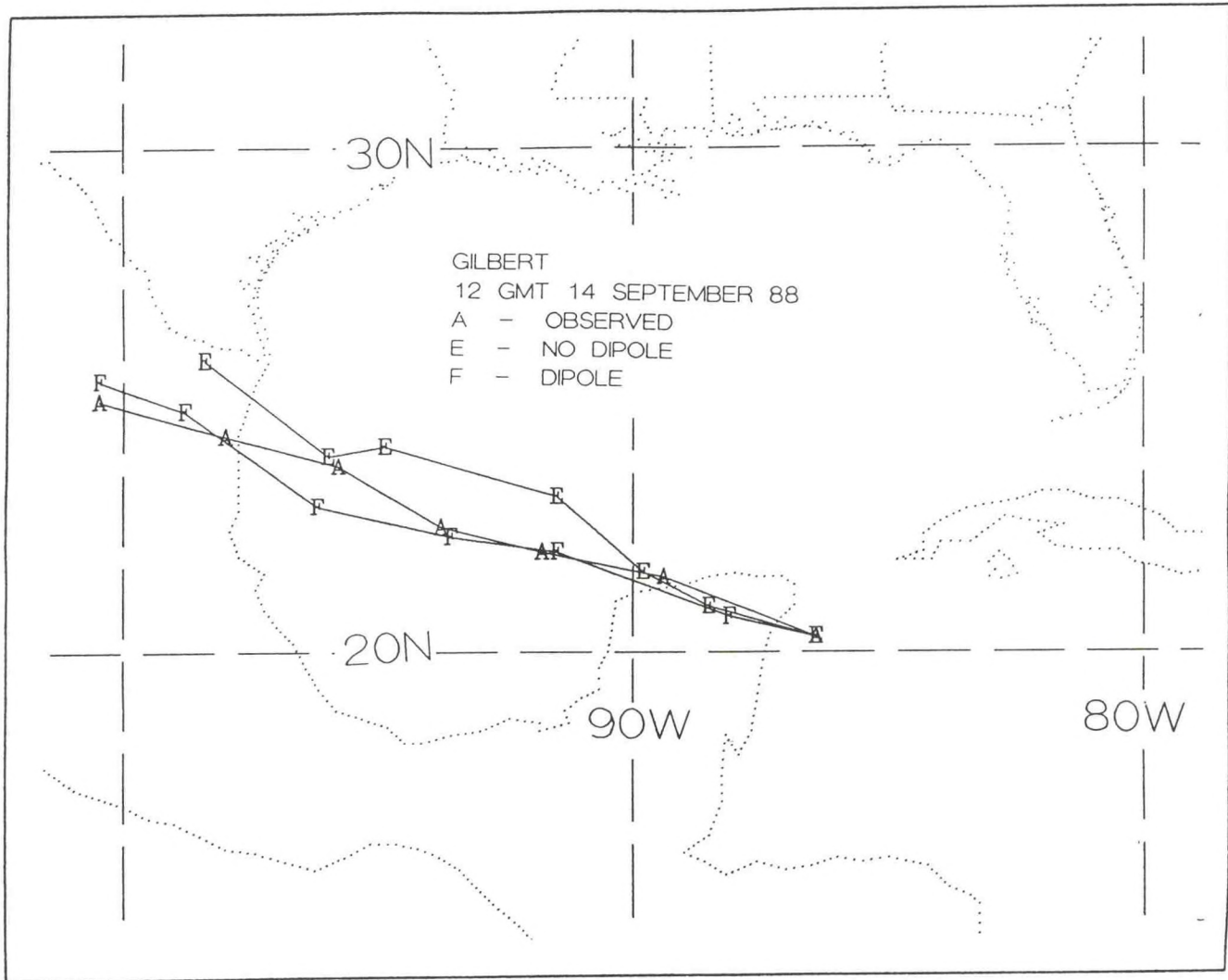


FIG. 2. Observed (A) and QLM predicted storm tracks (without (E) and with (F) a dipole) for Gilbert. Initial time is 12 GMT 14 Sept. 1988. Subsequent locations are shown at 12 hour intervals. $r_{max} = 740$ km, $c_{lat} = 20.3N$ (operational position).

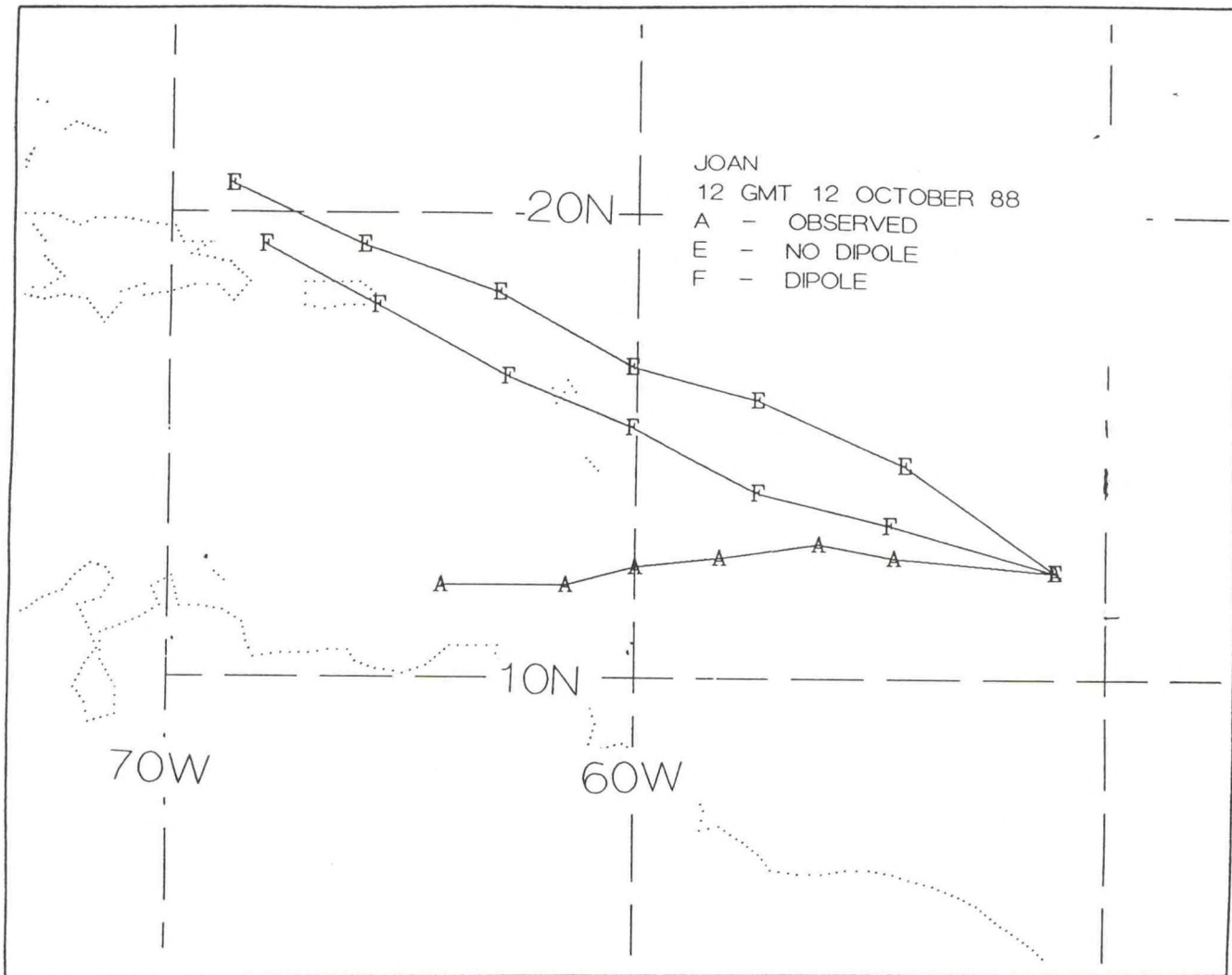


FIG. 3. Observed (A) and QLM predicted storm tracks (without (E) and with (F) a dipole) for Joan. Initial time is 12 GMT 12 Oct. 1988. Subsequent locations are shown at 12 hour intervals. $r_{\max} = 170$ km, $c_{lat} = 12.3N$ (operational position).

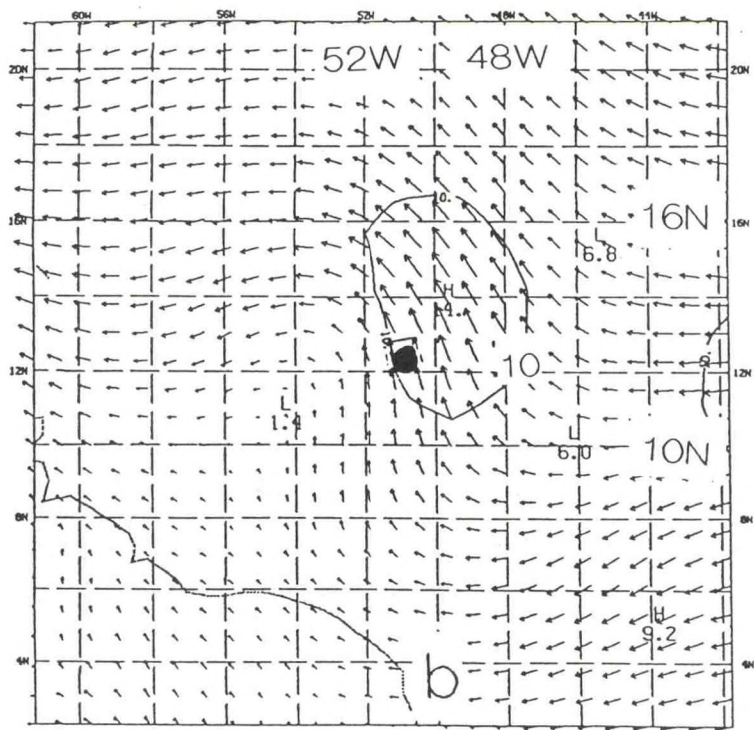
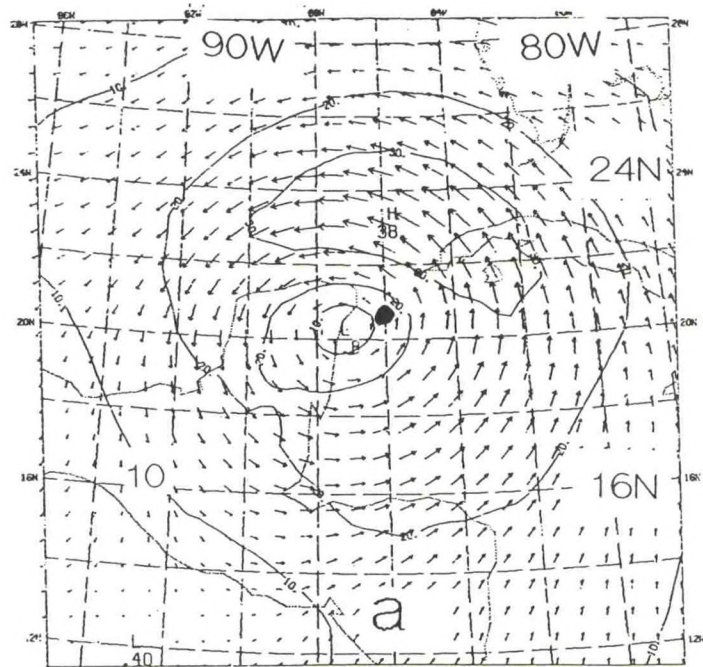


FIG. 4. Wind analysis (AVN) at 700 mb for (a) Gilbert at 12 GMT 14 Sept. 1988, and (b) Joan at 12 GMT 12 Oct. 1988. Observed location of the storm is shown by a heavy dot.

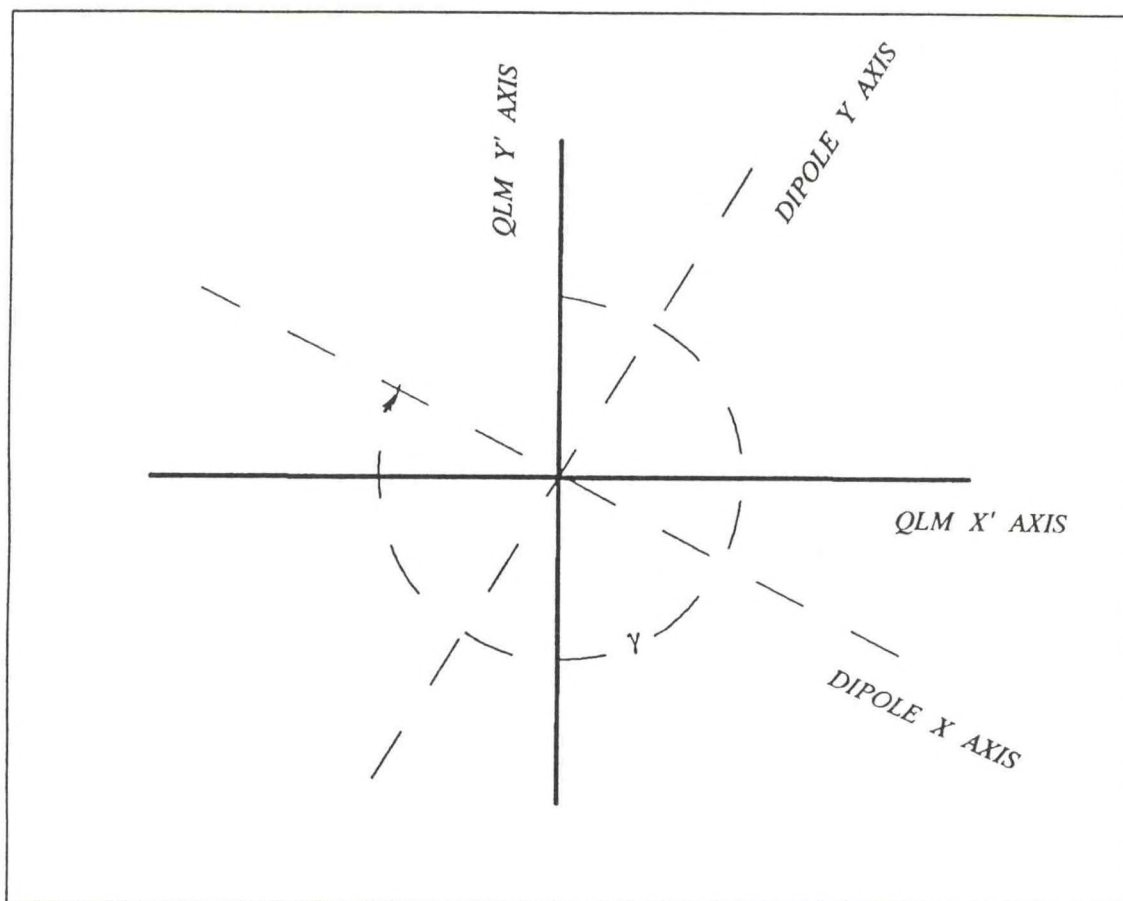


FIG. 5. Relative orientation of dipole and QLM axes.

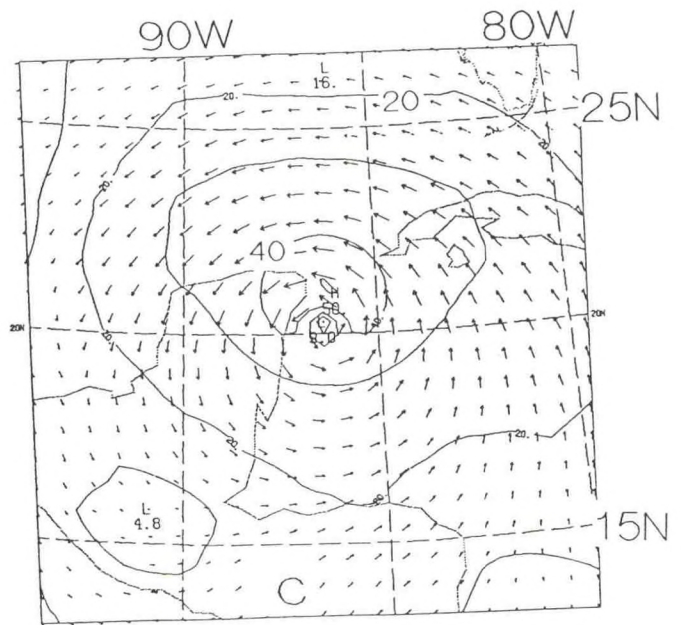
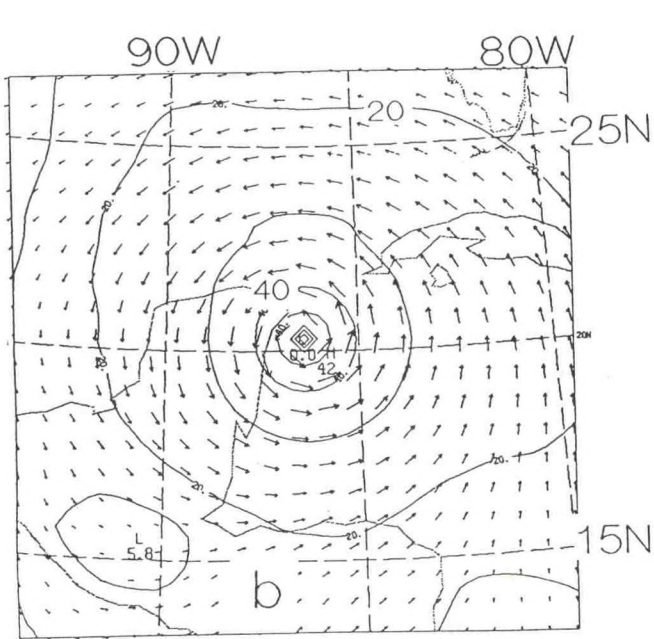
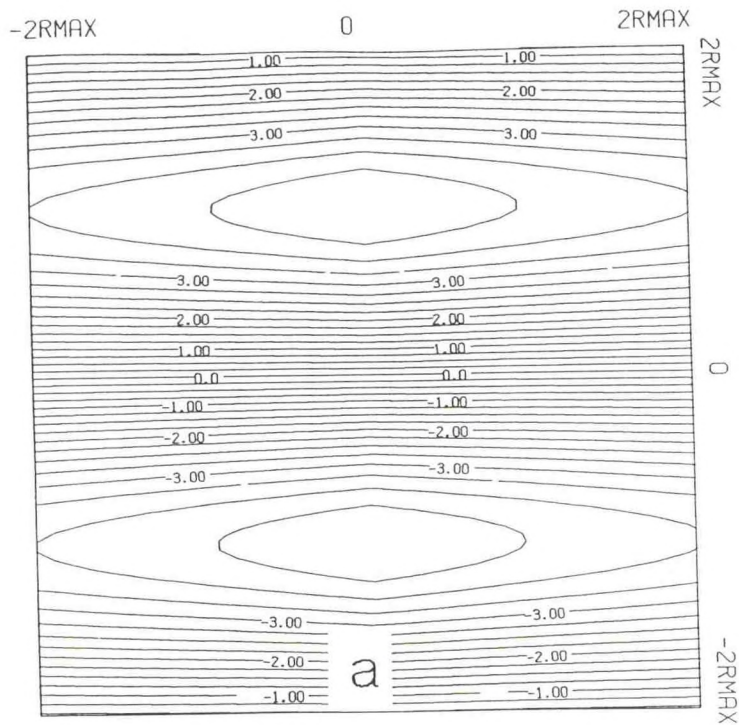


FIG. 6. Dipole structure for Gilbert at 12 GMT 14 Sept. 1988: (a) dipole streamfunction. Winds at 850 mb without (b) and with (c) a dipole. $r_{max} = 740$ km.

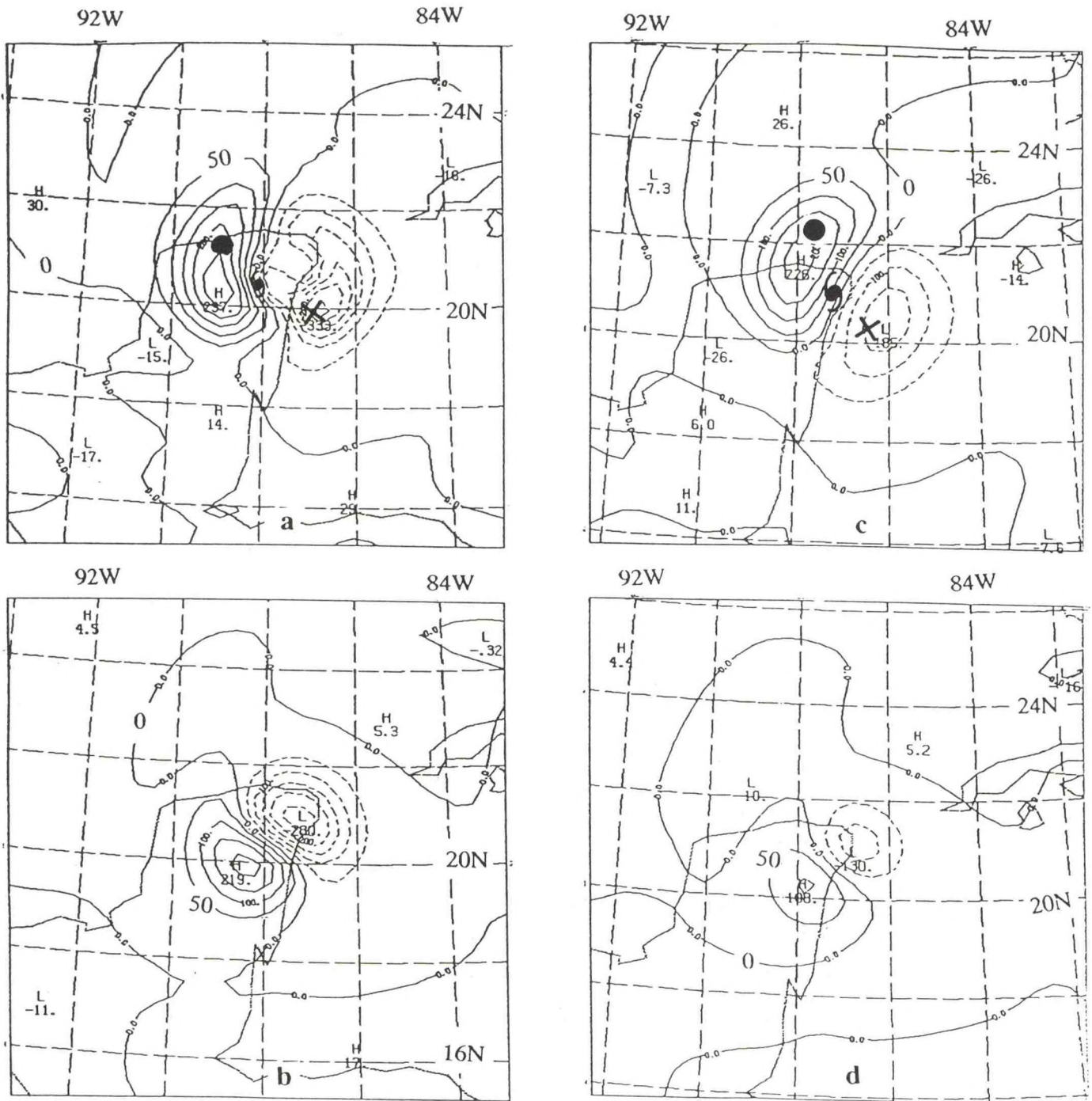


Fig. 7. 850 mb vorticity tendency terms: (a) total, and (b) stretching term in dipole case. (c) Total and (d) stretching term in no dipole case. Units: 10^{-10} s^{-2} . The location of maximum and minimum in horizontal advection term are shown by a heavy dot and a cross respectively in (a) and (c).

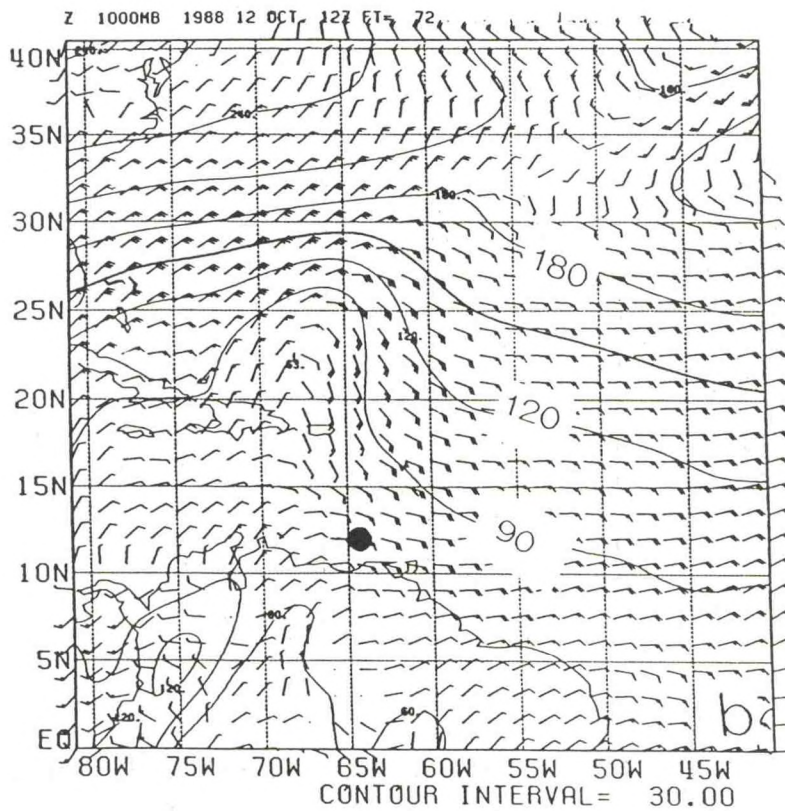
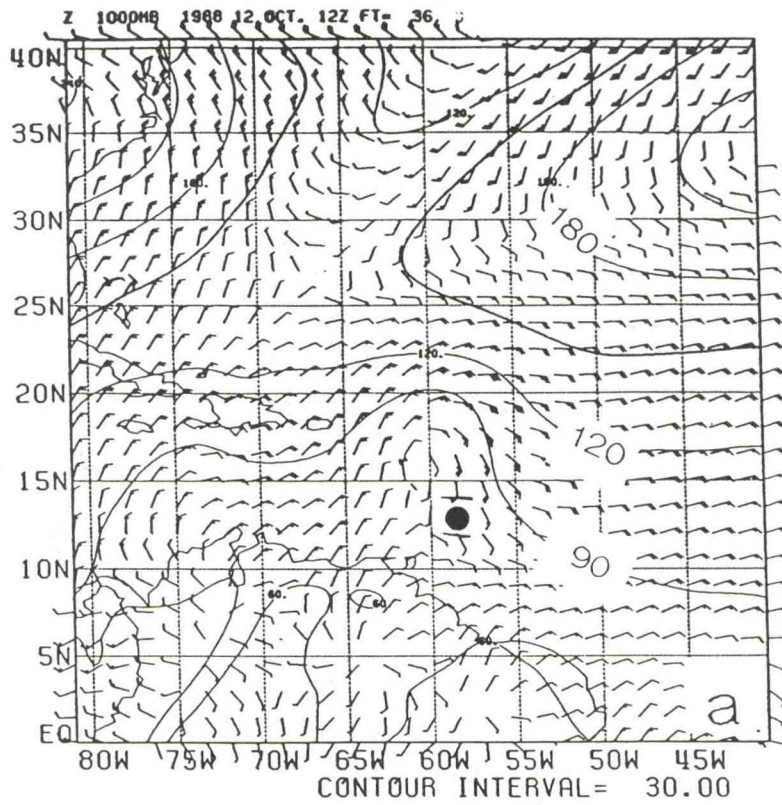


FIG. 8. AVN 1000 mb wind forecast for Joan, initial time 12 GMT 12 Oct.: (a) 36 h (b) 72 h. Observed location of the storm is shown by a heavy dot.

(continued from inside front cover)

NOAA Technical Memorandums

- NWS NMC 53 A Semi-Implicit Version of the Shuman-Hovermale Model. Joseph P. Gerrity, Jr., Ronald D. McPherson, and Stephen Scolnik, July 1973, 44 pp. (COM-73-11323)
- NWS NMC 54 Status Report on a Semi-Implicit Version of the Shuman-Hovermale Model. Kenneth Campana, March 1974, 22 pp. (COM-74-11096/AS)
- NWS NMC 55 An Evaluation of the National Meteorological Center's Experimental Boundary Layer Model. Paul D. Polger, December 1974, 16 pp. (COM-75-10267/AS)
- NWS NMC 56 Theoretical and Experimental Comparison of Selected Time Integration Methods Applied to Four-Dimensional Data Assimilation. Ronald D. McPherson and Robert E. Kistler, April 1975, 62 pp. (COM-75-10882/AS)
- NWS NMC 57 A Test of the Impact of NOAA-2 VTPR Soundings on Operational Analyses and Forecasts. William D. Bonner, Paul L. Lemar, Robert J. Van Haaren, Armand J. Desmarais, and Hugh M. O'Neil, February 1976, 43 pp. (PB-256-075)
- NWS NMC 58 Operational-Type Analyses Derived Without Radiosonde Data from NIMBUS 5 and NOAA 2 Temperature Soundings. William D. Bonner, Robert Van Haaren, and Christopher M. Hayden, March 1976, 17 pp. (PB-256-099)
- NWS NMC 59 Decomposition of a Wind Field on the Sphere. Clifford H. Dey and John A. Brown, Jr. April 1976, 13 pp. (PB-265-422)
- NWS NMC 60 The LFM Model 1976: A Documentation. Joseph P. Gerrity, Jr., December 1977, 68 pp. (PB-279-419)
- NWS NMC 61 Semi-Implicit Higher Order Version of the Shuman-Hovermale Model. Kenneth A. Campana, April 1978, 55 pp. (PB-286-012)
- NWS NMC 62 Addition of Orography to the Semi-Implicit Version of the Shuman-Hovermale Model. Kenneth A. Campana, April 1978, 17 pp. (PB-286-009)
- NWS NMC 63 Day-Night Differences in Radiosonde Observations in the Stratosphere and Troposphere. Raymond M. McInturff, Frederick G. Finger, Keith W. Johnson, and James D. Laver, September 1979, 54 pp. (PB80 117989)
- NWS NMC 64 The Use of Drifting Buoy Data at NMC. David Wright, June 1980, 23 pp. (PB80 220791)
- NWS NMC 65 Evaluation of TIROS-N Data, January-June 1979. David Wright, June 1980, 21 pp. (PB80 220494)
- NWS NMC 66 The LFM II Model--1980. John E. Newell and Dennis G. Deaven, August 1981, 20 pp. (PB82 156845)
- NWS NMC 67 Gulf Stream System Landward Surface Edge Statistics. Stephen J. Auer, October 1983, 20 pp. (PB84 104314)
- NWS NMC 68 (REVISION 1) Compendium of Marine Meteorological and Oceanographic Products of the Ocean Products Center. David M. Feit, September 1986, 93 pp. (PB87 101812/AS)
- NWS NMC 69 An Evaluation of NESDIS TOVS Physical Retrievals Using Data Impact Studies. Clifford, H. Dey, Ralph A. Petersen, Bradley A. Ballish, Peter M. Caplan, Lauren L. Morone, H. Jean Thieboux and Glenn H. White (NMC); Henry E. Fleming, Anthony L. Reale, and Donbald G. Gray (Office of Res. and Applications, NESDIS); Mitchell D. Goldberg and Jamie M. Daniels (ST Systems Corp); June 1989, 54 pp.
- NWS NMC 70 The Beta and Advection Model for Hurricane Track Forecasting. Donald G. Marks, January 1992, 89 pp.

NOAA SCIENTIFIC AND TECHNICAL PUBLICATIONS

The National Oceanic and Atmospheric Administration was established as part of the Department of Commerce on October 3, 1970. The mission responsibilities of NOAA are to assess the socioeconomic impact of natural and technological changes in the environment and to monitor and predict the state of the solid Earth, the oceans and their living resources, the atmosphere, and the space environment of the Earth.

The major components of NOAA regularly produce various types of scientific and technical information in the following kinds of publications:

PROFESSIONAL PAPERS — Important definitive research results, major techniques, and special investigations.

CONTRACT AND GRANT REPORTS — Reports prepared by contractors or grantees under NOAA sponsorship.

ATLAS — Presentation of analyzed data generally in the form of maps showing distribution of rainfall, chemical and physical conditions of oceans and atmosphere, distribution of fishes and marine mammals, ionospheric conditions, etc.

TECHNICAL SERVICE PUBLICATIONS — Reports containing data, observations, instructions, etc. A partial listing includes data serials; prediction and outlook periodicals; technical manuals, training papers, planning reports, and information serials; and miscellaneous technical publications.

TECHNICAL REPORTS — Journal quality with extensive details, mathematical developments, or data listings.

TECHNICAL MEMORANDUMS — Reports of preliminary, partial, or negative research or technology results, interim instructions, and the like.



Information on availability of NOAA publications can be obtained from:

**NATIONAL TECHNICAL INFORMATION SERVICE
U. S. DEPARTMENT OF COMMERCE
5285 PORT ROYAL ROAD
SPRINGFIELD, VA 22161**

E/AI22
Library & Information
Services Division, NOAA
6009 Executive Blvd.
Rockville, MD 20852

I

